

Aus dem Institut für Biosynthese neuraler Strukturen
des Zentrums für Molekulare Neurobiologie Hamburg
des Universitätsklinikums Hamburg-Eppendorf
Direktorin: Frau Prof. Dr. Melitta Schachner

Quantitative Immunocytochemical Analysis of the Neocortex of the Tenascin-R
Deficient and Wild-type Mice: Effects of Genotype and Aging on Major Cell
Populations

Dissertation

zur Erlangung des Doktors der Medizin

dem Fachbereich Medizin der Universität Hamburg vorgelegt von

Nadine Salis
aus Hamburg

Hamburg 2006

Angenommen vom Fachbereich Medizin
Der Universität Hamburg am:

Veröffentlicht mit Genehmigung des Fachbereichs
Medizin der Universität Hamburg

Prüfungsausschuss, die/der Vorsitzende/r:

Prüfungsausschuss: 2. Gutachter/in:

Prüfungsausschuss: 3. Gutachter/in:

CONTENTS

1	INTRODUCTION.....	5
1.1	Structure, expression and function of TNR.....	5
1.2	The TNR deficient mouse.....	6
1.2.1	<i>Electrophysiology</i>	7
1.2.2	<i>Behaviour</i>	7
1.2.3	<i>Morphology</i>	8
2	RATIONALE AND AIMS OF THE STUDY.....	9
3	MATERIAL AND METHODS.....	10
3.1	Animals.....	10
3.2	Tissue preparation for morphological analyses.....	10
3.3	Antibodies.....	11
3.4	Immunofluorescence staining.....	14
3.5	Stereological analysis.....	14
3.6	Evaluation of cortical thickness.....	15
3.7	Photographic images.....	15
3.8	Statistical analysis.....	16
4	RESULTS.....	17
4.1	Morphological analyses of the motor cortex.....	17
4.1.1	<i>Cortical thickness and total cell population</i>	17
4.1.2	<i>Neuronal and glial cells</i>	18
4.1.3	<i>Inhibitory interneurons</i>	22
4.2	Morphological analyses of the sensory cortex.....	26
4.2.1	<i>Cortical thickness and total cell population</i>	26
4.2.2	<i>Neuronal and glial cells</i>	27
4.2.3	<i>Inhibitory interneurons</i>	29

5	DISCUSSION.....	32
5.1	Genotype-related aberrations in adult mice.....	34
5.2	Age-related changes in old TNR deficient mice.....	36
5.3	Age-related changes independent of genotype.....	37
5.4	Possible functional significance of the structural aberrations in TNR deficient mice.....	38
6	SUMMARY.....	39
7	REFERENCES.....	41
8	ABBREVIATIONS.....	45
9	ACKNOWLEDGEMENT/DANKSAGUNG.....	47
10	CURRICULUM VITAE.....	48
11	EIDESSTÄTTLICHE VERSICHERUNG.....	49

1 INTRODUCTION

1.1 Structure, expression and functions of tenascin-R

Tenascin-R (TNR) is an extracellular matrix protein expressed primarily in the central nervous system by oligodendrocytes and neuronal subpopulations (Erickson, 1993; Bartsch *et al.*, 1993; Fuss *et al.*, 1993; Schachner *et al.*, 1994). It belongs to the tenascin family of proteins and its genomic structure spans 85 kb and contains 21 exons (Fig. 1). Compared with tenascin-C (TNC) and tenascin-X (TNX), two members of the tenascin family, the positions of the introns are conserved (Leprini *et al.*, 1996). TNR has a cysteine-rich N-terminal region, followed by 4.5 epidermal growth factor like (EGFL) domains, 8 fibronectin type III (FNIII) like repeats and a fibronogen-homologous C-terminus (Jones and Jones, 2000). Two isoforms, with molecular weight of 160 kD and 180 kD, are generated by alternative splicing of the sixth FNIII domain (Pesheva *et al.*, 1989).



Figure 1: Genomic structure of TNR: spans 85 kb and contains 21 exons.

During the brain development, TNR is first detectable around birth. It is expressed by oligodendrocyte progenitors and type-2 astrocytes and is most abundant during the phase of active myelination. After myelination has ceased TNR levels are down-regulated to lower adult levels (Bartsch *et al.*, 1993; Wintergerst *et al.*, 1993). In adult rodents, TNR is produced by and detectable in the extracellular matrix (perineuronal nets) around motor neurons in the spinal cord and brain stem, as well as interneurons and in the cerebellum, hippocampus and olfactory bulb. Furthermore, TNR is present at nodes of Ranvier of myelinated axons and on outer aspects of myelin sheaths in adult animals (Bartsch *et al.*, 1993).

In the olfactory bulb, TNR-positive immunostaining is restricted to the granule cells and the internal plexiform layer (Saghatelian *et al.*, 2004).

In vitro, TNR supports the adhesion of oligodendrocytes and enhances oligodendrocyte process formation (Pesheva *et al.*, 1997). Its effects on neurons depend on the way it is presented to the cultured cells. TNR inhibits neurite outgrowth when present as a substrate boundary on a permissive uniform substrate but enhances outgrowth as an uniform growth substrate (Pesheva *et al.*, 1994; Schachner *et al.*, 1994, Faissner 1997, Becker *et al.*, 2000).

In vivo and in vitro studies in the recent years have clearly indicated that TNR is an important modulator of plasticity and repair processes in the CNS. TNR regulates inhibitory perisomatic inhibition via interactions of its HNK-1 (human natural killer cell) carbohydrate epitope with GABA_B receptors and thus influences synaptic transmission and plasticity in the hippocampus (Brenneke *et al.*, 2004; Bukalo *et al.*, 2001; Dityatev and Schachner, 2003; Saghatelian *et al.*, 2000, 2001). In myelinated CNS axons, TNR is a functional modulator of the beta-subunit of voltage-gated sodium channels (Xiao *et al.*, 1999; Srinivasan *et al.*, 1998). TNR has also inhibitory functions in the outgrowth and guidance of optic axons in vivo (Becker *et al.*, 1999; Becker *et al.*, 2003; Becker *et al.*, 2004). Also, it has been observed that TNR influences a variety of microglial functions such as cell adhesion, migration and secretion of cytokines and growth factors (Angelov *et al.*, 1998; Liao *et al.*, 2005). After spinal cord injury, TNR expression is upregulated in the lesion area (Deckner *et al.*, 2000) and it has been suggested TNR is among the oligodendrocyte-derived molecules inhibiting axonal regrowth after SCI (Pesheva and Probstmeier, 2000; Sandvig *et al.*, 2004).

1.2 The TNR deficient mouse

TNR deficient mice have been created and initial analyses have revealed that they are vital and fertile, have a normal life span and no gross anatomical or histological abnormalities (Weber *et al.*, 1999). However, the structure of the perineuronal nets is abnormal in the knockout mice and the action potential conduction velocity is reduced compared to wild-type mice (Weber *et al.*, 1999).

Further studies have identified structural, physiological and behavioural abnormalities in the TNR deficient mouse.

1.2.1 Electrophysiology

Synaptic transmission and plasticity in the hippocampus of TNR deficient mice are abnormal as compared to wild-type mice in several respects (Saghatelian *et al.*, 2001): long term potentiation (LTP) is reduced in the CA1 region, basal excitatory synaptic transmission in synapses formed on CA1 pyramidal cell bodies is increased and the amplitude of unitary inhibitory postsynaptic currents (IPSC) evoked by stimulation of perisomatic interneurons is reduced by factor of two. The frequency of failures in γ -aminobutyric acid (GABA) release is increased. The reduction of the LTP induced by theta-burst stimulation of Schaffer collaterals of the stratum radiatum is smaller in TNR deficient compared with wild-type mice (Bukalo *et al.*, 2001). Upon repetitive stimulation of Schaffer collaterals at 1 Hz, the number of secondary spikes are significantly increased in the stratum radiatum of the CA1 region in the hippocampus of TNR deficient mice (Brenneke *et al.*, 2004).

A recent study of EEG and auditory evoked potentials (AEPs) in the hippocampal CA1 field and cortex has revealed differences between TNR deficient and wild-type mice (Gurevicius *et al.*, 2004). The hippocampal gamma oscillations (frequency range 30 – 80 Hz) are significantly enhanced in amplitude, the cortical EEG signals are increased in amplitude over a wide frequency range (2 – 40 Hz) and the amplitude of the cortical AEPs is almost doubled in TNR deficient compared to wild-type mice.

All these findings have lead to the conclusion that TNR is involved in inhibitory mechanisms in the brain.

1.2.2 Behaviour

Compared to wild-type mice TNR deficient mice have no obvious abnormalities in their general appearance. They appear healthy and their body weight is normal during early adulthood. However, at the age of 11 month the TNR

deficient mice become slightly but significantly heavier than wild-type mice (Freitag *et al.*, 2003).

TNR deficient mice spend more time resting and less time eating and drinking, appear less motivated in several tests, explore the environment less actively and are more anxious.

The TNR deficient mice perform poorly in motor coordination tests such as pole, wire-hanging and rotarod tests (Freitag *et al.*, 2003; Montag-Sallaz and Montag, 2003).

Finally, a two-way active avoidance test (shuttle box) has indicated a deficit in associative learning in TNR deficient mice.

1.2.3 Morphology

The perisomatic coverage of the pyramidal neurons in the CA1 region of the hippocampus with inhibitory synapses, estimated as number of symmetric active zones per unit length of the cell surface, is reduced by more than 40% in TNR deficient mice and the individual active zones are smaller than in wild-type mice (Nikonenko *et al.*, 2003). In addition, the spatial arrangement of pyramidal cell bodies is more diffuse in TNR deficient mice compared with wild-type littermates (Nikonenko *et al.*, 2003). It has been shown that TNR deficient mice have lower numbers of calretinin-positive neurons and more glial fibrillary acidic protein (GFAP)-immunoreactive astrocytes in the hippocampus compared to wild-type littermates (Brenneke *et al.*, 2004).

2 RATIONALE AND AIMS OF THE STUDY

A number of behavioural and physiological abnormalities have been identified in TNR deficient mice but the origins of most of these anomalies are not known. This study addressed the question as to whether TNR deficiency causes structural aberrations in the cerebral cortex that may underlie abnormal behavioural traits and brain functions. With a view to previous experience with versatile morphometric and stereological analyses (Irintchev *et al.*, 2005), the motor and sensory cortices were selected for this study. It is based on immunohistochemical visualization of defined cell types (total neuronal population, interneuron subpopulations, astrocytes, oligodendrocytes and microglia) and stereological estimation of cell densities and volumes of structures. The particular aims of these investigation were to determine whether:

1. TNR deficiency causes changes in the cortical thickness in the somatosensory and motor areas of the neocortex
2. major cell populations are normally formed and maintained in size throughout life in the absence of TNR

In order to answer the second question, both adult (5 months of age) old (18 – 22 months) TNR deficient mice and wild-type littermates were included in the study.

3 MATERIALS AND METHODS

3.1 Animals

Wild-type (TNR+/+) mice and TNR deficient (TNR-/-) littermates obtained the SPF (specific pathogen-free) facility of the Universitätsklinikum Hamburg (UKE) and originated from original TNR colony (Weber *et al.*, 1999). Seven TNR+/+ mice and 8 TNR-/- littermates were studied at the age of 5 months (referred to as adult mice). Six animals per genotype were analysed at the age of 18 – 20 months (old mice). All animals had healthy appearance before sacrifice for morphological investigations. Body weight was similar in TNR deficient and wild-type mice: 32 ± 3.3 g (mean \pm standard deviation) *versus* 33 ± 3.2 g and 32 ± 3.6 g *versus* 34 ± 5.5 g in TNR+/+ *versus* TNR-/- animals studied at the age of 5 and 18 months, respectively ($p > 0.05$, two-sided *t* tests for independent groups). The genotype of the mutant mice had been determined in advance by polymerase chain reaction (PCR; Weber *et al.*, 1999). Animals treatments were performed in accordance to the German law for protection of experimental animals. All technical procedures described below were performed according to Irintchev *et al.* (2005).

3.2 Tissue preparation for morphological analyses

The mice were anaesthetized by intraperitoneal injections of 16% solution of sodium pentobarbital (Narcoren®, Merial, Hallbermoos, Germany, $5 \mu\text{l g}^{-1}$ body weight) and transcardially perfused with physiologic saline for 60 seconds and fixative (4% w/v formaldehyde and 0.1% CaCl_2 in 0.1M cacodylate buffer, pH 7.3, 15 minutes at room temperature, RT). The brains were dissected out without the olfactory bulbs and post-fixed overnight for 18 to 22 hours 4°C in the formaldehyde solution used for perfusion supplemented with 15% w/v sucrose. After that, the tissue was immersed in 15% sucrose solution in 0.1M cacodylate buffer, pH 7.3, for additional 24 hours.

After this fixation and cryoprotection (sucrose infiltration) the brains were placed into a mouse brain matrix (World Precision Instruments, Berlin, Germany) and cut through the most caudal slot of the matrix (i.e., close to the caudal pole of the

cerebellum). Following the cut, the tissue was frozen for two minutes in 2-methylbutane (isopentane) precooled to -30°C in the cryostat.

Serial coronal sections of $25\ \mu\text{m}$ thickness were cut in caudal-to-rostral direction on a cryostat (Leica CM3050, Leica Instruments, Nußloch, Germany). Sections were picked up on a series of 10 SuperFrost®Plus glass slides (Roth, Karlsruhe, Germany), so that 4 sections 250 μm apart were present on each slide. The sections were air-dried at RT for at least 1 hour and stored in boxes at -20°C until used for immunohistochemical stainings.

3.3 Antibodies

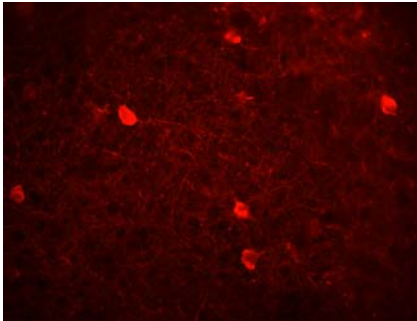
Commercially available antibodies were used at optimal dilutions as indicated in Table 1.

Antibody	Abbreviation	Clone	Producer	Dilution
anti parvalbumin	anti-PV	mouse monoclonal, clone: Parv 19	Sigma, Deisenhofen, Germany	1:1000, 9.8 µg/ml Ig
anti-neuron specific nuclear antigen	anti-NeuN	mouse monoclonal, clone: A60	Sigma	1:1000, 1 µg/ml Ig
anti-cyclic nucleotide phosphatase	anti-CNP	mouse monoclonal, clone; 11-5B	Sigma	1:1000, 7.5 µg/ml Ig
anti-S100	anti-S100	rabbit polyclonal, purified IgG fraction	DakoCytomation, Hamburg, Germany	1:500, 9 µg/ml Ig
anti-Iba-1	anti-Iba-1	Rabbit polyclonal, affinity purified	Wako Chemicals, Neuss, Germany	1:1500, 0.3 µg/ml Ig
anti-calbindin	anti-CB	rabbit polyclonal, affinity purified	Sigma	1:1000, 0.5 µg/ml Ig
anti-calretinin	anti-CR	rabbit polyclonal, affinity purified	Sigma	1:250, 3.2 µg/ml Ig

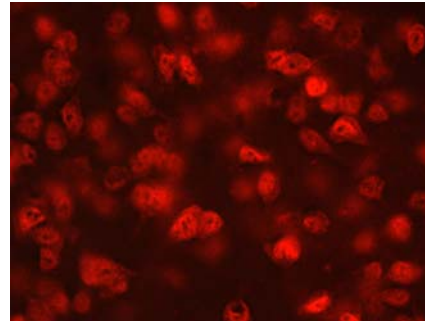
Table 1: Commercially available antibodies shown with abbreviation, clone, producer and used dilution.

Figure 2: Examples of immunohistochemical stainings in sections of TNR+/+ and TNR -/- in the motor cortex

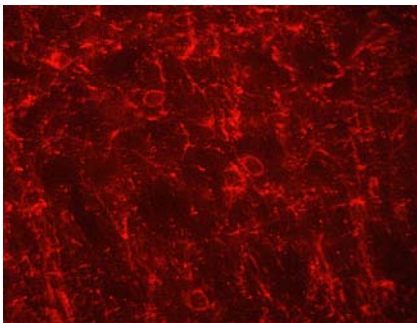
A: anti PV



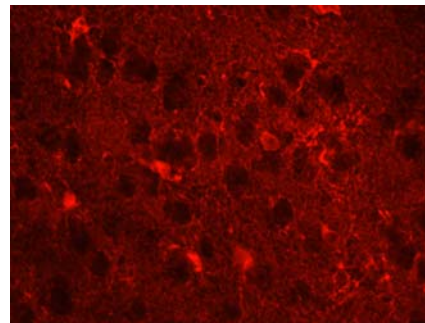
B: anti NeuN



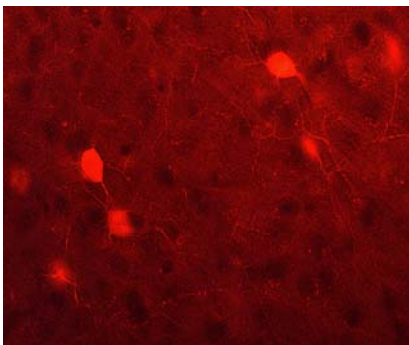
C: anti CNP



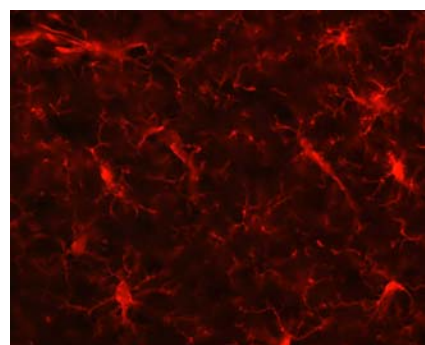
D: anti S100



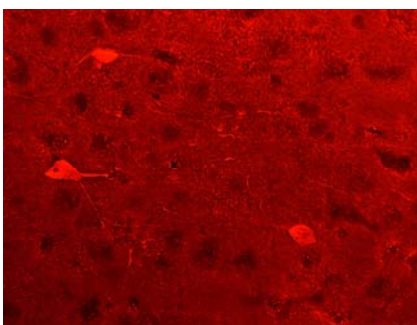
E: anti CB



F: anti Iba1



G: anti CR



3.4 Immunofluorescence staining

The basis for the immunofluorescence staining was a method described by Sofroniew and Schrell (1982) as modified by Irintchev *et al.* (1993; 1994; 1998, 2005). The method allows the repeated use of antibody solutions (stabilized by the non-gelling vegetable gelatin lambda-carrageenan), is convenient because all incubations are performed in jars and is characterized by high reproducibility.

Brain sections, stored at -20°C , were air-dried at 37°C for 30 minutes and immersed for antigen de-masking into 0.01 M sodium citrate solution (pH 9.0, adjusted with 0.01 M NaOH) pre-heated to 80°C in a water bath for 30 minutes (Jiao *et al.*, 1999).

After the cooling of the slides to room temperature phosphate-buffered saline (PBS, pH 7.3) solution containing 0.2% Triton X-100, 0.02% sodium azide and 5% normal goat serum was applied for 1 hour at RT to the sections to block non-specific binding sites. Without rinsing, the sections were incubated for 3 days at 4°C with the primary antibody diluted in PBS containing 0.5% lambda-carrageenan and 0.02% sodium azide. Afterwards the slides were washed (3 x 15 minutes at RT). Appropriate secondary antibody, diluted 1:200 in PBS-carrageenan solution, was applied for 2 hours at RT.

Goat anti-rabbit or goat anti-mouse IgG conjugated with Cy3 (Jackson Immuno Research Laboratories, Dianova, Hamburg, Germany) were used.

After washing in PBS cell nuclei were stained for 10 minutes at RT with bis-benzimide solution (Hoechst 33258 dye, $5\ \mu\text{g ml}^{-1}$ in PBS, Sigma), the slides were washed again and the sections were mounted under coverslips using an anti-fading medium (Fluoromount G, Southern Biotechnology Associates, Biozol, Eching, Germany). The sections were stored in the dark at 4°C .

3.5 Stereological analysis

The optical disector method (Gundersen, 1986) was utilized to estimate numerical cell densities. Counting was performed on an Axioskop microscope (Zeiss, Oberkochen, Germany) equipped with a motorized stage and a Neurolucida software-controlled computer system (MicroBrightField Europe, Magdeburg, Germany).

Per animal and staining, four spaced-serial sections 250 µm apart, collected at distances of 7 to 8 mm rostral from the caudal pole of the cerebellum (see cutting procedure above), were analysed.

By viewing the nuclear staining at a low magnification (Plan-Neofluar® 10x/0.3 objective), the agranular motor cortex and the granular sensory cortex could be identified as described (Irintchev *et al.*, 2005) and outlined on the Neurolucida screen projected onto the microscope visual field.

Counting on immunolabeled cell nuclei was carried out within systematically randomly spaced optical disectors throughout the outlined cortical areas.

The following technical parameters were used during quantifications: guard space depth 2 µm, base and height of the disector 3600 µm² and 10 µm, respectively distance between the optical disectors 60 µm for the motor cortex and 90 µm for the sensory cortex, objective 40x Plan-Neofluar® 40x/0.75. Four to eight fields of the motor and the sensory cortex in the left or right hemisphere were analysed per animal and staining. All analyses were performed blindly on coded preparations.

3.6 Evaluation of cortical thickness

For determination of the average cortical thickness, the area of the delineated field was divided by the length of its boundary facing the meningeal surface (Irintchev *et al.*, 2005).

3.7 Photographic images

For the photographic documentation, an Axiophot 2 microscope equipped with a digital camera AxioCam HRC and AxioVision software (Zeiss) was used. Adobe® Photoshop® 6.0 software (Adobe Systems Inc., San Jose, California) was used to process the images.

3.8 Statistical analysis

Group mean values were compared using two-sided t test for independent samples or analysis of variance with subsequent Tukey post-hoc test and, SigmaStat 2.0 software (SPSS, Chicago, Illinois). The accepted level of significance was set at 5%.

4 RESULTS

4.1 Morphological analyses of the motor cortex

4.1.1 Cortical thickness and total cell population

The normalized cortical thickness (Fig. 3) of the motor cortex showed an age-related decrease in the cortical volume. However, there were no genotype-specific differences between TNR^{-/-} and TNR^{+/+} mice at both ages.

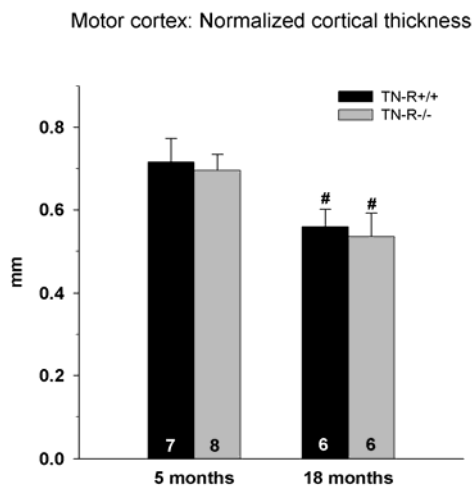


Figure 3: Normalized thickness of the motor cortex in TNR^{+/+} (black bars) and TNR^{-/-} animals (grey bars) studied at the age of 5 and 18 months. Shown are mean values + SD. The number of animals studied per group is indicated at the base of each bar. Cross-hatches indicate significant differences compared with adult (5-month-old) mice ($p < 0.05$, analysis of variance, ANOVA, and Tukey post-hoc tests).

There was no difference in the total cell density, as evaluated by counting of all nuclei, between TNR^{-/-} and TNR^{+/+} mice as well as no age-related changes (Fig. 4). Since cortical thickness was reduced in old compared to adult mice of both genotypes, for this and all other parameters in the motor cortex, cell numbers per column (column: cortical tissue under 1 mm² cortical surface) were calculated. Total number of cells was significantly reduced in both genotypes at the age of 18 – 20 months compared to adult (5-month-old) mice indicating absolute cell loss with age (Fig. 5).

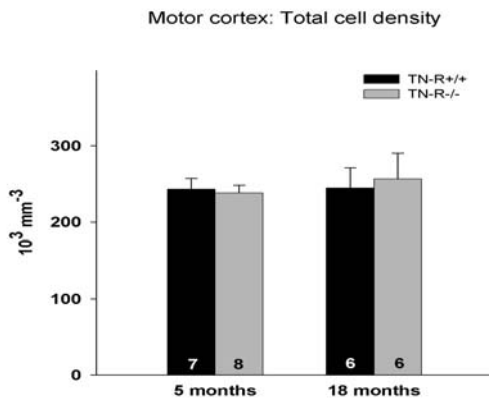


Figure 4: Numerical densities of all cells, identified by nuclear staining, in the motor cortex of TNR+/+ (black bars) and TNR-/- animals (grey bars) studied at the age of 5 and 18 months. Shown are mean values + SD. The number of animals studied per group is indicated at the base of each bar. No significant differences among the groups were found (ANOVA).

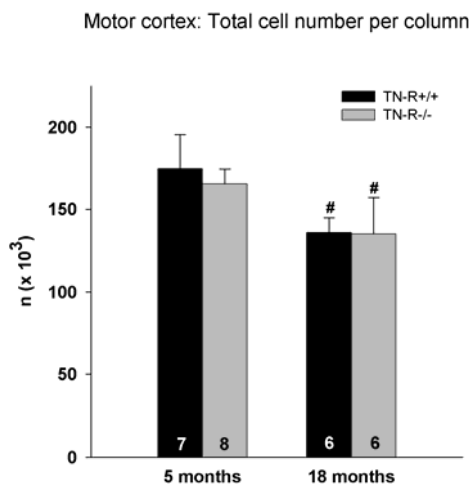


Figure 5: Total numbers of cells per column (cortical tissue under 1mm² cortical surface) in the motor cortex in the motor cortex of TNR+/+ (black bars) and TNR-/- animals (grey bars) studied at the age of 5 and 18 months. Shown are mean values + SD. The number of animals studied per group is indicated at the base of each bar. Cross-hatches indicate significant differences compared with adult (5-month-old) mice ($p < 0.05$, analysis of variance, ANOVA, and Tukey post-hoc tests).

4.1.2 Neuronal and glial cells

No differences among the groups of animals were found for densities of cells positive for NeuN, a marker expressed by all neurons in the neocortex (Fig. 6).

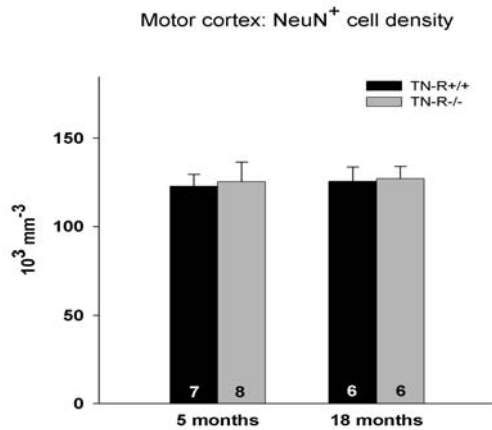


Figure 6: Numerical densities of all neurons, identified by NeuN staining, in the motor cortex of TNR^{+/+} (black bars) and TNR^{-/-} animals (grey bars) studied at the age of 5 and 18 months. Shown are mean values + SD. The number of animals studied per group is indicated at the base of each bar. No significant differences among the groups were found (ANOVA).

Because of the age-related decline in the cortical thickness, numbers of NeuN-positive cells per column were significantly reduced in old TNR^{-/-} and TNR^{+/+} mice compared with the groups of adult mice (Fig. 7). Thus, independent of genotype, there was a significant loss of neurons with age.

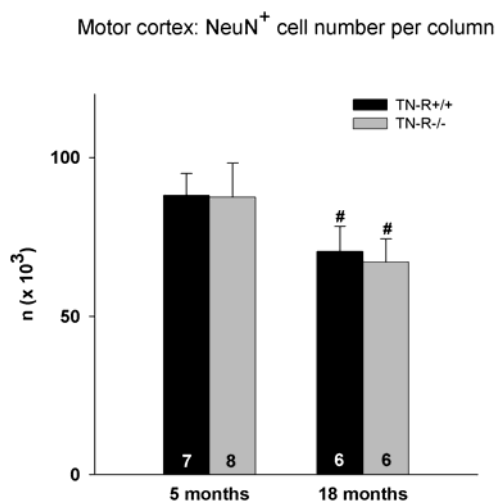


Figure 7: Numbers of NeuN-positive neurons per column (cortical tissue under 1 mm² cortical surface) in the motor cortex of TNR^{+/+} (black bars) and TNR^{-/-} animals (grey bars) studied at the age of 5 and 18 months. Shown are mean values + SD. The number of animals studied per group is indicated in the base of each bar. Cross-hatches indicate significant differences compared with adult (5-month-old) mice ($p < 0.05$, analysis of variance, ANOVA, and Tukey post-hoc tests).

Genotype-related differences in numbers of S-100-positive astrocytes, calculated per unit volume cortical column, were not found (Fig. 8 and Fig. 9). In contrast to neurons, no absolute loss of astrocytes was found with age (Fig. 9).

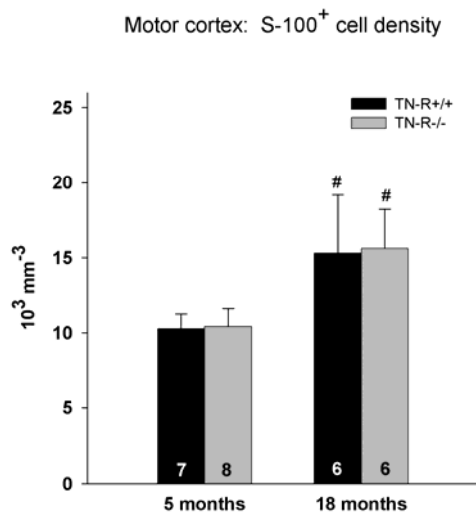


Figure 8: Numerical densities of S-100-positive astrocytes in the motor cortex of TNT^{+/+} (black bars) and TNR^{-/-} animals (grey bars) studied at the age of 5 and 18 months. Shown are mean values + SD. The number of animals studied per group is indicated at the base of each bar. Cross-hatches indicate significant differences compared with adult (5-month-old) mice ($p < 0.05$, analysis of variance, ANOVA, and Tukey post-hoc tests).

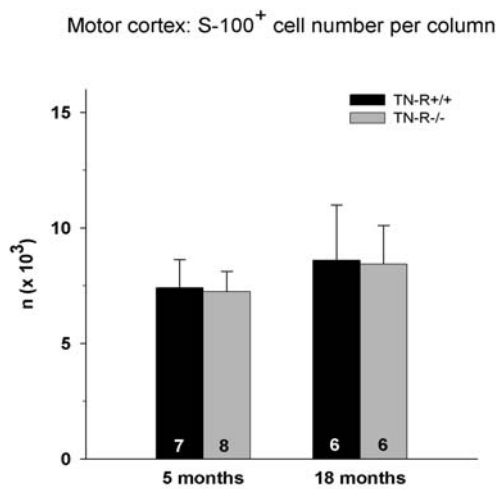


Figure 9: Numbers of S-100-positive astrocytes per column in the motor cortex of TNR^{+/+} (black bars) and TNR^{-/-} animals (grey bars) studied at the age of 5 and 18 months. Shown are mean values + SD. The number of animals studied per group is indicated at the base of each bar. No significant differences among the groups were found (ANOVA).

Numbers of CNPase-positive oligodendrocytes per column were similar in all 4 groups (Fig. 11) and densities differed significantly only between adult and old TNR^{+/+} mice (Fig. 10). Therefore, there were no significant effects of genotype and age on the size of the oligodendrocyte population.

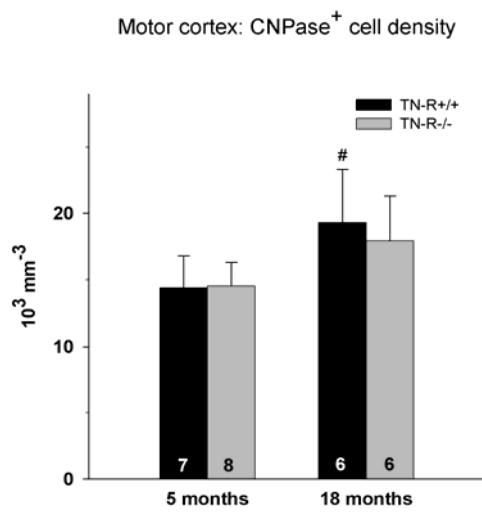


Figure 10: Numerical densities of CNPase-positive oligodendrocytes in the motor cortex of TNR^{+/+} (black bars) and TNR^{-/-} animals (grey bars) studied at the age of 5 and 18 months. Shown are values + SD. The number of animals studied per group is indicated in the base of each bar. Cross-hatches indicate significant differences compared with adult (5-month-old) mice ($p < 0.05$, analysis of variance, ANOVA, and Tukey post-hoc tests).

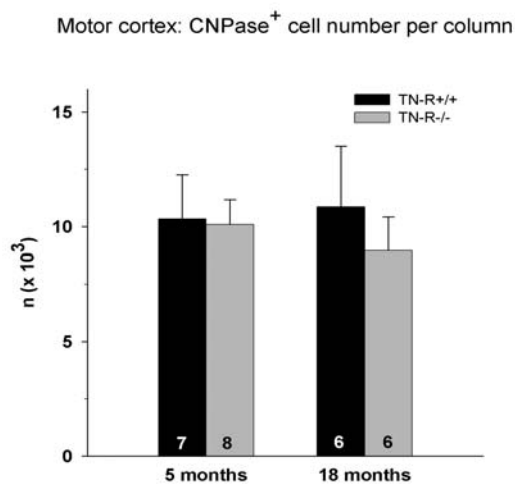


Figure 11: Numbers of CNPase-positive oligodendrocytes per column (cortical tissue under 1 mm² cortical surface) in the motor cortex of TNR^{+/+} (black bars) and TNR^{-/-} animals (grey bars) studied at the age of 5 and 18 months. Shown are mean values + SD. The number of animals studied per group is indicated at the base of each bar. No significant differences among the groups were found (ANOVA).

Similar to neurons, numbers of Iba-1-positive microglial cells were significantly reduced with age in both TNR^{-/-} and TNR^{+/+} mice and no differences were found between age-matched groups of different genotype (Fig. 12 and Fig. 13).

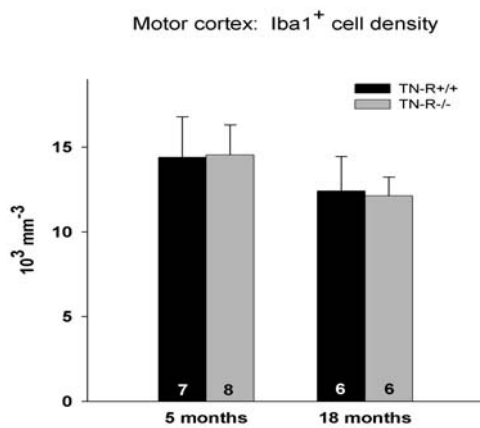


Figure 12: Numerical densities of Iba1-positive microglial cells in the motor cortex of TNR^{+/+} (black bars) and TNR^{-/-} animals (grey bars) studied at the age of 5 and 12 months. Shown are mean values + SD. The number of animals studied per group is indicated at the base of each bar. No significant differences among the groups were found (ANOVA).

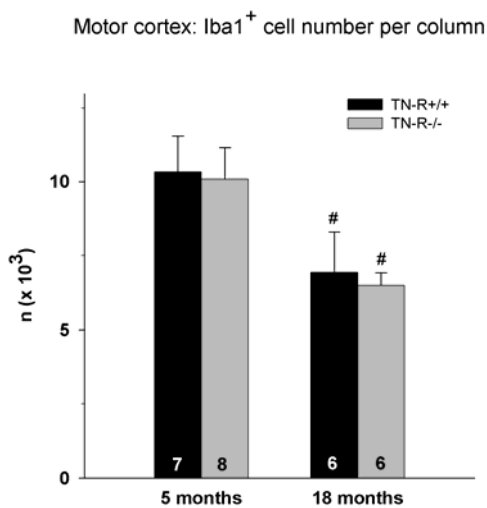


Figure 13: Numbers of Iba1-positive microglial cells per column (cortical tissue under 1 mm² cortical surface) in the motor cortex of TNR^{+/+} (black bars) and TNR^{-/-} animals (grey bars) studied at the age of 5 and 18 months. Shown are mean values + SD. The number of animals studied per group is indicated at the base of each bar. Cross-hatches indicate significant differences compared with adult (5-month-old) mice ($p < 0.05$, analysis of variance, ANOVA, and Tukey post-hoc tests).

4.1.3 Inhibitory interneurons

Numbers of PV-positive interneurons, calculated both per unit volume and per column, were significantly reduced in old compared to adult TNR^{+/+} mice (Figs. 14 and 15). In contrast, densities of PV-positive neurons were similar in adult and old TNR^{-/-} mice and numbers per column were no significantly reduced with age in TNR^{-/-} mice. Therefore, lack of TNR causes an attenuation of the age-

related loss of PV-positive interneurons characteristic of aging in genetically normal mice.

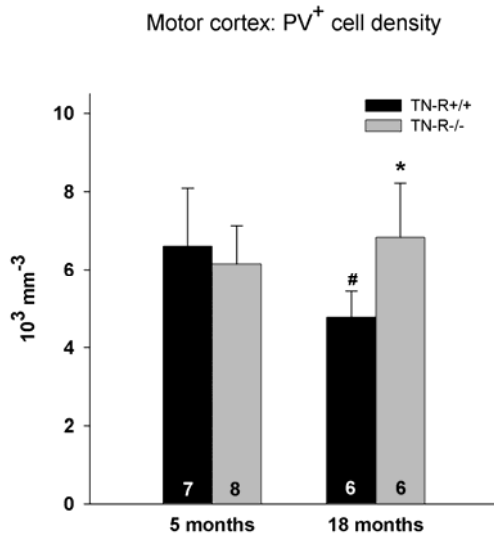


Figure 14: Numerical densities of PV-positive interneurons in the motor cortex of TNR^{+/+} (black bars) and TNR^{-/-} animals (grey bars) studied at the age of 5 and 18 months. Shown are mean values + SD. The number of animals studied per group is indicated at the base of each bar. Cross-hatch and asterisk indicate significant differences compared with adult (5-month-old) TNR^{+/+} and old TNR^{+/+} mice, respectively ($p < 0.05$, analysis of variance, ANOVA, and Tukey post-hoc tests).

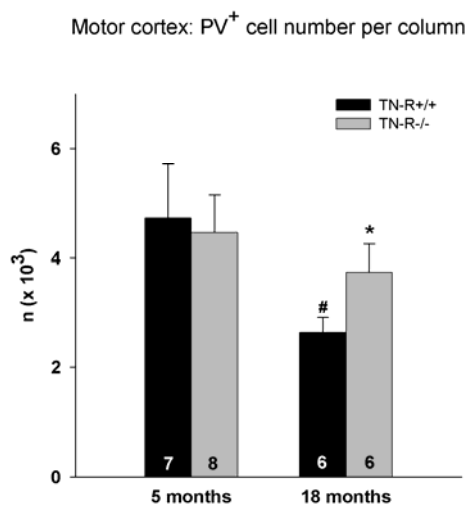


Figure 15: Numbers of PV-positive interneurons per column (cortical tissue under 1 mm² cortical surface) in the motor cortex of TNR^{+/+} (black bars) and TNR^{-/-} animals (grey bars) studied at the age of 5 and 18 months. Shown are mean values + SD. The number of animals studied per group is indicated at the base of each bar. Cross-hatch and asterisk indicate significant differences compared with adult (5-month-old) TNR^{+/+} and old TNR^{+/+} mice, respectively ($p < 0.05$, analysis of variance, ANOVA, and Tukey post-hoc tests).

Densities and numbers per column of CB-positive interneurons were similar among old TNR+/+ and adult TNR+/+ and TNR-/- mice (Figs. 16 and 17). Age- and genotype-specific loss of CB-positive neurons was found in old TNR-/- mice (Figs. 16 and 17).

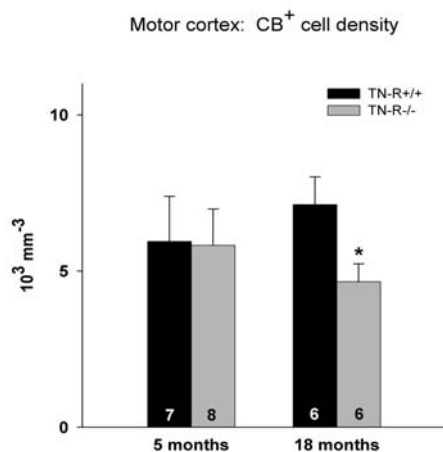


Figure 16: Numerical densities of CB-positive interneurons in the motor cortex of TNR+/+ (black bars) and TNR-/- animals (grey bars) studied at the age of 5 and 18 months. Shown are mean values + SD. The number of animals studied per group is indicated at the base of each bar. Asterisk indicates significant difference compared with the age-matched group (ANOVA and Tukey post-hoc test).

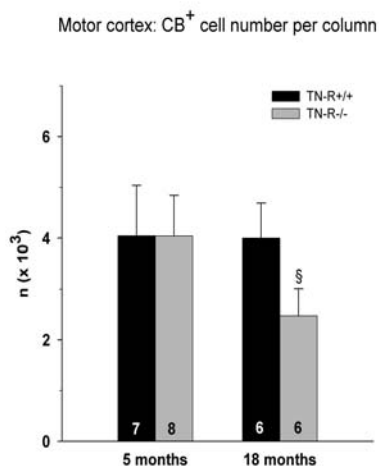


Figure 17: Numbers of CB-positive interneurons per column (cortical tissue under 1 mm² cortical surface) in the motor cortex of TNR+/+ (black bars) and TNR-/- animals (grey bars) studied per group at the age of 5 and 18 months. Shown are mean values + SD. The number of animals studied per group is indicated at the base of each bar. Section sign (§) indicates significant differences from all other groups (ANOVA and Tukey post-hoc tests).

Specific deficit, as evaluated by both densities and number per column, in the CR-positive interneurons was found in adult TNR^{-/-} mice compared with age-matched TNR^{+/+} mice (Figs. 18 and 19). Age-related differences were not observed.

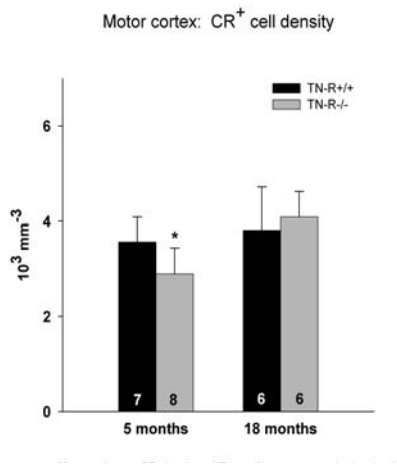


Figure 18: Numerical densities of CR-positive interneurons in the motor cortex of TNR^{+/+} (black bars) and TNR^{-/-} animals (grey bars) studied at the age of 5 and 18 months. Shown are mean values + SD. The number of animals studied per group is indicated at the base of each bar. Asterisk indicates significant differences as compared to the age-matched group (ANOVA and Tukey post-hoc test).

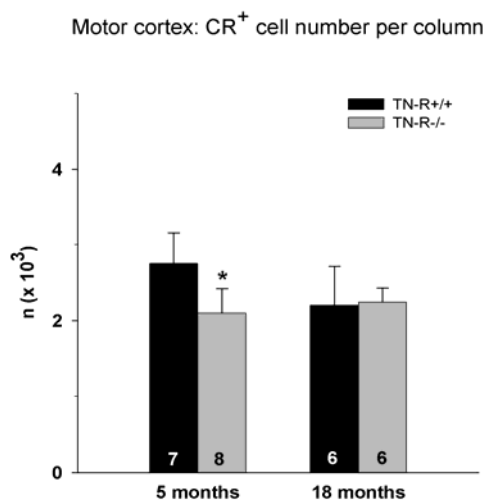


Figure 19: Number of CR-positive interneurons per column (cortical tissue under 1 mm² cortical surface) in the motor cortex of TNR^{+/+} (black bars) and TNR^{-/-} animals (grey bars) studied at the age of 5 and 18 months. Shown are mean value + SD. The number of animals studied per group is indicated at the base of each bar. Asterisk indicates significant differences as compared to the age-matched group (ANOVA and Tukey post-hoc test).

4.2 Morphological analyses of the sensory cortex

4.2.1 Cortical thickness and total cell population

In contrast to the motor cortex, the normalized thickness of the sensory cortex decreased with age in neither TNR^{-/-} or TNR^{+/+} mice (Fig. 20). Similar to the motor cortex, there were no genotype-related differences. All data for the sensory cortex are presented as cell densities because, at similar thickness of the cortex in all groups, densities reflect numbers of cells per column to a similar degree for all groups.

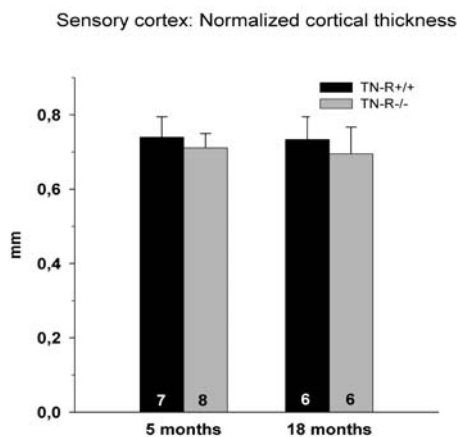


Figure 20: Normalized thickness of the sensory cortex in TNR^{+/+} (black bars) and TNR^{-/-} animals (grey bars) studied at the age of 5 and 18 months. Shown are mean values + SD. The number of animals studied per group is indicated at the base of each bar. No significant differences among the groups were found (ANOVA).

The total cell density in sensory cortex was affected by neither genotype nor age (Fig. 21).

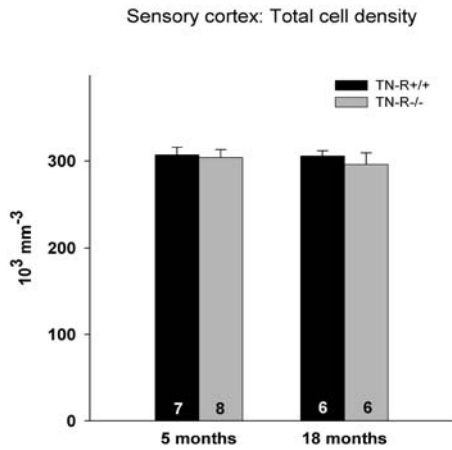


Figure 21: Numerical densities of all cells, identified by nuclear staining, in the sensory cortex of TNR+/+ (black bars) and TNR-/- animals (grey bars) studied at the age of 5 and 18 months. Shown are mean values + SD. The number of animals studied per group is indicated at the base of each bar. No significant differences among the groups were found (ANOVA).

4.2.2 Neuronal and glial cells

Similar to the motor cortex, no effects of genotype on the numbers of NeuN-positive neurons was found in the sensory cortex and, for both genotypes, an age-related decline in neuronal numbers was observed (Fig. 22). The age-related loss of neurons was, however, smaller in the sensory compared to the motor cortex (compare Figs. 22 and 7).

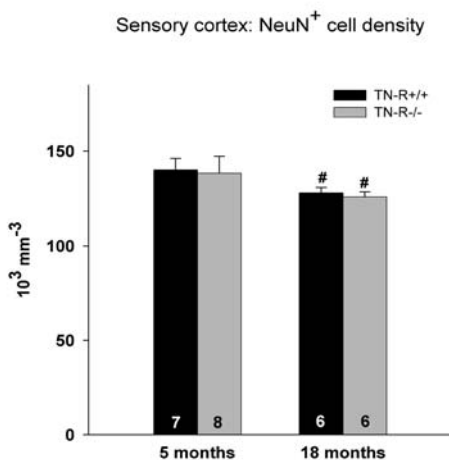


Figure 22: Numerical densities of all neurons, identified by NeuN staining, in the sensory cortex of TNR+/+ (black bars) and TNR-/- animals (grey bars) studied at the age of 5 and 18 months. Shown are mean values + SD. The number of animals studied per group is indicated at the base of each bar. Cross-hatches indicate significant differences compared with adult (5-month-old) mice ($p < 0.05$, analysis of variance, ANOVA, and Tukey post-hoc tests).

For all types of glial cell studied, S-100-positive astrocytes (Fig. 23), CNPase-positive oligodendrocytes (Fig. 24) and microglial cells (Fig. 25), cell numbers did not differ among the groups indicating neither age- nor genotype-specific impacts on the glial populations in the sensory cortex.

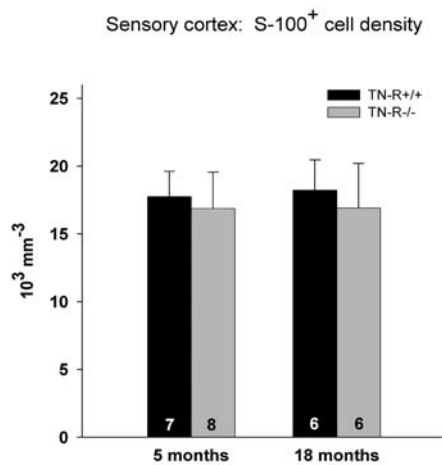


Figure 23: Numerical densities of S-100-positive astrocytes in the sensory cortex of TNR^{+/+} (black bars) and TNR^{-/-} animals (grey bars) studied at the age of 5 and 18 months. Shown are mean values + SD. The number of animals studied per group is indicated at the base of each bar. No significant differences among the groups were found (ANOVA).

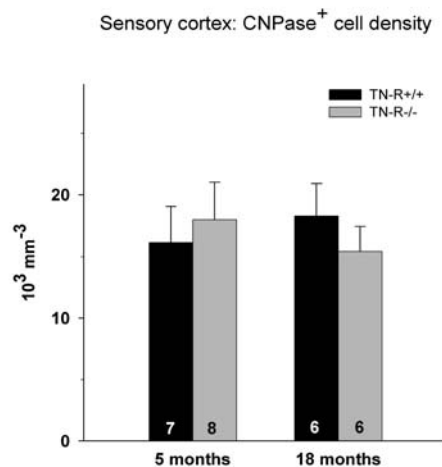


Figure 24: Numerical densities of CNPase-positive oligodendrocytes in the sensory cortex of TNR^{+/+} (black bars) and TNR^{-/-} animals (grey bars) studied at the age of 5 and 18 months. Shown are mean values + SD. The number of animals studied per group is indicated at the base of each bar. No significant differences among the groups were found (ANOVA).

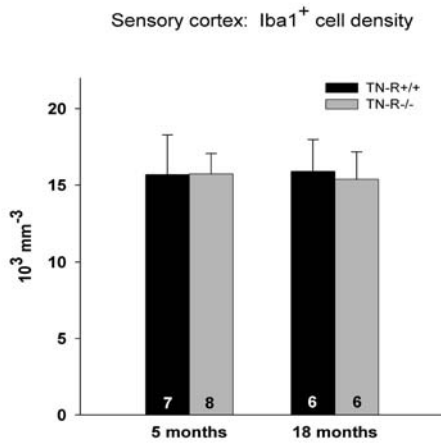


Figure 25: Numerical densities of Iba1-positive microglial cells in the sensory cortex of TNR^{+/+} (black bars) and TNR^{-/-} animals (grey bars) studied at the age of 5 and 12 months. Shown are mean values + SD. The number of animals studied per group is indicated at the base of each bar. No significant differences among the groups were found (ANOVA).

4.2.3 Inhibitory interneurons

Numbers of PV-positive interneurons were similar in age-matched groups indicating no effect of the TNR deficiency on this subpopulation of interneurons (Fig. 26). Decline with age was prominent in both genotypes. In contrast, in the motor cortex such decline was observed only in wild-type mice.

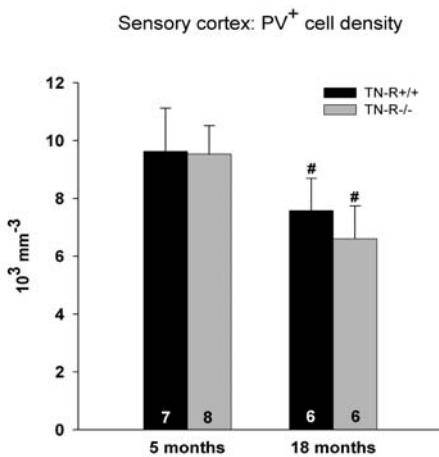


Figure 26: Numerical density of PV-positive interneurons in the sensory cortex of TNR^{+/+} (black bars) and TNR^{-/-} animals (grey bars) studied at the age of 5 and 18 months. Shown are mean values + SD. The number of animals studied per group is indicated at the base of each bar. Cross-hatches indicate significant differences compared with adult (5-month-old) mice ($p < 0.05$, analysis of variance, ANOVA, and Tukey post-hoc tests).

No significant differences were found among the groups for densities of CB-positive interneurons (Fig. 27). Similar to the motor cortex, a tendency for lower numbers of CB neurons in the old TNR^{-/-} compared with old TNR^{+/+} mice ($p < 0.05$, two-sided t test for independent samples, not significant in a more stringent ANOVA test with Tukey's multiple comparisons).

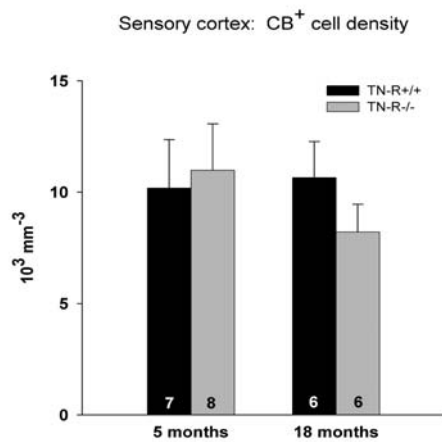


Figure 27: Numerical densities of CB-positive interneurons in the sensory cortex of TNR^{+/+} (black bars) and TNR^{-/-} animals (grey bars) studied at the age of 5 and 18 months. Shown are mean values + SD. The number of animals studied per group is indicated in the base of each bar. No significant differences among the groups were found (ANOVA).

As in the motor cortex, the only significant difference observed for CR-positive interneurons in the sensory cortex was a reduction in cell numbers, as compared with age-matched animals, in adult TNR^{-/-} mice (Fig. 28).

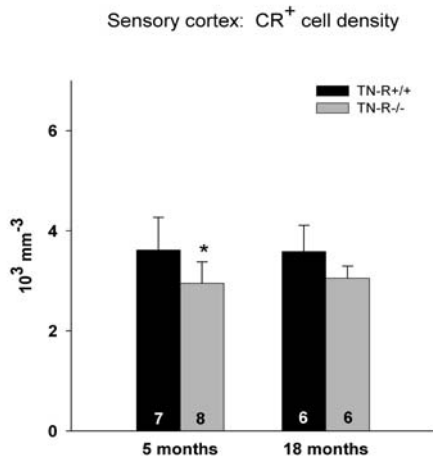


Figure 28: Numerical densities of CR-positive interneurons in the sensory cortex of TNR+/+ (black bars) and TNR-/- animals (grey bars) studied at the age of 5 and 18 months. Shown are mean values + SD. The number of animals studied per group is indicated at the base of each bar. Asterisk indicates significant difference as compared to the age-matched group (ANOVA and Tukey post-hoc test).

5 DISCUSSION

This study provides first quantitative data on major cell populations in the cerebral cortex of TNR-deficient mice. A brief overview of the results is given in Table 2. Analyses of mice at two different ages, 5 months (adult mice) and 18 – 20 months (old mice) led to identification of genotype- and age-related changes in major cell populations allowing conclusions about the importance of TNR for the formation and structural maintenance of the cerebral cortex. Moreover, the consequences of aging in wild-type littermates, i.e. in genetically normal laboratory mice, could be precisely analysed.

Table 2: Summary of age- and phenotype-related differences.

Parameter / Cell type	Genotype-related differences TNR ^{-/-} versus TNR ^{+/+}		Age-related differences 18 months versus 5 months	
	5 months	18 months	TNR ^{+/+}	TNR ^{-/-}
		Motor cortex *		
Thickness	=	=	↓ (-22%)	↓ (-23%)
All cells	=	=	↓ (-21%)	↓ (-18%)
All neurons	=	=	↓ (-29%)	↓ (-29%)
PV ⁺ neurons	=	↑ (+29%)	↓ (-44%)	=
CB ⁺ neurons	=	↓ (-38%)	=	=
CR ⁺ neurons	↓ (-20%)	=	=	=
Oligodendrocytes	=	=	=	=
Astrocytes	=	=	=	=
Microglia	=	=	↓ (-33%)	↓ (-35%)
		Sensory cortex *		
Thickness	=	=	=	=
All cells	=	=	=	=
All neurons	=	=	↓ (-10%)	↓ (-10%)
PV ⁺ neurons	=	=	↓ (-20%)	↓ (-31%)
CB ⁺ neurons	=	= (-23% [#])	=	=
CR ⁺ neurons	↓ (-19%)	= (-19% [#])	=	=
Oligodendrocytes	=	=	=	=
Astrocytes	=	=	=	=
Microglia	=	=	=	=

Statistically significant (↑,↓) and non-significant (=) differences (ANOVA and post hoc Tukey test) between group mean values. Numbers in brackets indicate the difference in percent between the two mean values. PV – parvalbumin; CB – calbindin; CR – calretinin. * Comparisons are based on numbers of cells per column in the motor cortex and cell densities for the sensory cortex. [#]

Significant difference in a t test, but not in the more stringent Tukey multiple-comparison test.

5.1 Genotype-related aberrations in adult mice

Analyses of cortical thickness, total cell and total neuronal numbers, as well as numbers of parvalbumin- and calbindin-positive interneurons, and of oligodendrocytes and astrocytes did not reveal differences between TNR^{-/-} and TNR^{+/+} mice (Table 2). From these findings it can be concluded that TNR deficiency does not influence the formation, maturation and maintenance of the major cell populations in the mouse cortex. Also, numbers of microglial cells, a sensitive indicator of neurodegenerative processes, were normal in the cortex of the TNR^{-/-} animals. The quantitative observations in this study are in agreement with previous qualitative analyses suggesting that major brain structures such as the hippocampus, cerebellum and spinal cord are normally developed in the TNR - deficient mouse (Weber *et al.*, 1999). The lack of pronounced developmental abnormalities in the TNR knockout mouse are explainable by the relative late onset of TNR expression in the mouse and restriction of this expression to a few cell populations. In the mouse brain, TNR becomes detectable at birth and high levels of TNR expression by oligodendrocyte progenitors and oligodendrocytes are associated with myelination in the central nervous system (CNS) (Bartsch *et al.*, 1993; Wintergerst *et al.*, 1993). After myelination has ceased, TNR expression is reduced but the protein remains detectable at the nodes of Ranvier in the adult mouse brain (Bartsch *et al.*, 1993). Since myelin structure (Weber *et al.*, 1999) and numbers of oligodendrocytes (this study) in the TNR deficient mouse are normal, TNR does not appear to be essential for the formation and maintenance of myelin or myelin-producing cells.

During postnatal development and in adulthood, TNR is also expressed by interneurons in the cerebral cortex, cerebellum, hippocampus, spinal cord and retina, as well as motoneurons in the spinal cord (Fuss *et al.*, 1993; Wintergerst *et al.*, 1993; Weber *et al.*, 1999). TNR is accumulated in perineuronal nets surrounding these neurons (Adams *et al.*, 2001; Brückner *et al.*, 2000; Wintergerst *et al.*, 1996). In the cerebral cortex of rodents, the vast majority (94 - 98%) of the cells surrounded by perineuronal nets, and thus expressing TNR, are parvalbumin-positive interneurons (Fuss *et al.*, 1993; Wegner *et al.*, 2003; Irintchev *et al.*, 2005; Carulli *et al.*, 2006). And similar to oligodendrocytes that also express TNR, the size of the parvalbumin-positive cell population in TNR deficient mice was normal at 5 months of age. Previous observations have suggested that the populations of

PV-positive interneurons in the somatosensory cortex, retrosplenial cortex and the hippocampus of THN^{-/-} mice are also normal (Brenneke *et al.* 2004; Saghatelian *et al.*, 2001; Weber *et al.*, 1999). Parvalbumin-positive interneurons, coupled both chemically and electrically, form an inhibitory cortical network operating at high-frequency discharge rates which is of major importance for basic cortical properties such as synchronization and oscillatory activities (Fukuda and Kosaka, 2000; Galarreta and Hestrin, 2002; Freund, 2003). Mice deficient in TNR have impaired inhibition and enhanced cortical evoked potentials (Saghatelian *et al.*, 2001; Gurevicius *et al.*, 2004). The finding of normal numbers of parvalbumin-positive cells in this study indicates that enhanced excitability of the neocortex of TNR deficient mice is not related to deficiency in this major subpopulation of interneurons. Rather, similar to the hippocampus of TNR deficient mice, cortical hyperexcitability might be related to reduced perisomatic inhibition of principal neurons (Saghatelian *et al.*, 2001; Nikonenko *et al.*, 2003).

Regarding the lack of effects of mutation on cell populations that normally express TNR, it was surprising to find significant reductions in the numbers of calretinin-positive (and TNR-negative) interneurons in both the motor and sensory cortices of TNR deficient mice (about -20% compared to wild-type littermates, Table 2). The calretinin-positive neurons in the neocortex and hippocampus are known as interneuron-specific cells meaning that they predominantly form inhibitory synaptic contacts on other types of interneuron such as, for example, parvalbumin- or calbindin-positive interneurons (Somogyi and Klausberger, 2005). The interpretation of the observed deficit of calretinin-positive interneurons in functional terms is difficult since the precise functional role of this type of interneurons is not known. It can be speculated that, because of exerting influences on interneurons that shape the synchronous activity of excitatory cortical output neurons, small changes in the numbers of these cells may have significant impacts on the spontaneous and evoked electrical activity in the neocortex which might contribute to the known physiological abnormalities in the cortex and hippocampus of TNR deficient mice.

5.2 Age-related changes in old TNR deficient mice

By including old TNR^{-/-} mice and wild-type littermates (18 – 20 months), in addition to adult animals (5 months), the hypothesis was tested that possible compensatory mechanisms limiting the impacts of constitutive TNR deficiency during development and adulthood may become deficient at old age. Populations of interneurons appeared to be specifically affected by aging of TNR deficient mice. Numbers of calbindin-positive cells, which were not affected by aging in TNR^{+/+} mice, were significantly reduced in the motor cortex of old TNR^{-/-} mice (-39% compared to TNR^{+/+} littermates) and the same tendency was found for the sensory cortex (-23%, Table 2). Parvalbumin-positive interneurons were significantly more numerous in the motor cortex of old TNR^{-/-} mice compared with TNR^{+/+} littermates (+29%, Table 2). This difference was due to age-related loss of parvalbumin-positive neurons in TNR^{+/+} mice, but not in TNR^{-/-} littermates (Table 1, see also 5.3). In the sensory cortex, however, no such apparent “sparing” of parvalbumin-positive interneurons was not found (Table 2) indicating that numbers of parvalbumin-positive interneurons are affected by aging in a cortical region-specific fashion in the TNR deficient mouse. The observed declines in cell numbers must not necessarily reflect loss of cells. These changes might be simply due to loss of expression of calcium binding proteins, parvalbumin or calbindin, which cannot be proved since other specific markers of the interneuron subpopulations studied here are not available. Even if only alterations in expression patterns occur, this would have functional consequences because calcium-buffering protein profiles are important for the specification of the firing patterns of interneuron subpopulations (Freund, 2003; Somogyi and Klausberger, 2005). Cell types other than interneurons were not specifically affected by aging in the TNR deficient mouse. Altogether, these findings support the hypothesis that compensatory mechanisms are exhausted with age in the TNR deficient mouse. The questions as to why such changes occur and why these are restricted to interneurons cannot be answered at present. The finding that both TNR expressing and non-expressing interneurons (parvalbumin- and calbindin-positive, respectively) are affected at old age suggests role(s) of TNR in maintaining cell circuitries rather than simply directly determining the size of cell populations normally expressing this protein.

5.3 Age-related changes independent of genotype

The results of this study show that aging, independent of genotype of the animals, affects the two neocortical areas studied, the sensory and the motor cortices, to different degrees. In the sensory cortex, a small age-related decline in the number of all neurons was found (-10% compared to adult mice for both genotypes, Table 2). More prominent, compared to the total neuronal population, was the reduction of parvalbumin-positive interneurons with age (-20% and -31% in TNR+/+ and TNR-/- mice, respectively, Table 2). Since parvalbumin-positive interneurons comprise only 5-7% of the total neuronal population in adult mice (compare Figs. 6 and 14 and Figs. 22 and 26) and most neurons, i.e. around 80%, in the mouse neocortex are excitatory (Irintchev *et al.*, 2005), it is apparent that the age-related loss of neurons affects both parvalbumin-positive inhibitory interneurons and excitatory neurons in the sensory cortex. Changes in other cell populations were not detected in the sensory cortex and also cortical thickness was not reduced with age. In the motor cortex, reduction in the numbers of all neurons in both old TNR-/- and TNR+/+ mice and of parvalbumin-positive interneurons in old TNR+/+ animals was also found (-29% for all neurons in both cortical areas and -44% for parvalbumin interneurons, Table 2). Loss of neurons was more pronounced in the motor cortex compared to the sensory cortex and this was accompanied by reduction of the cortical thickness and of all cells as well as of microglial cells in animals of both genotypes (-18 to -35% for different parameters and animal groups compared to respective values in adult mice, Table 2). These observations indicate that age-related loss of excitatory and inhibitory neurons and microglial cells does occur in the cortex of aging mice. However, different cortical areas are affected to different degrees suggesting different time-course of progression of the aberrations. Regarding neuronal numbers, the present findings are in agreement with the widely accepted view that age-related impairment of brain functions result from neuronal loss. Several stereological studies in the recent years, however, have challenged this view by showing that normal neuronal numbers are maintained in the neocortex, cerebellar cortex and hippocampus of aged rodents, primates and humans (Andersen *et al.*, 2003; Hof and Morrison, 2004; Long *et al.*, 1999; Morrison and Hof, 1997; Pakkenberg and Gundersen, 1997). In these “design-based” stereological analyses, for example the studies of Andersen *et al.*, 2003 and Pakkenberg and Gundersen, 1997, total

neuronal numbers per cerebellum or neocortex have been determined thus neglecting the functional heterogeneity of the cortical structures and the possibility that different areas are affected to varying degrees. The latter possibility was clearly demonstrated in this study indicating the necessity for analysing defined areas of the cortices rather than performing global counts. This conclusion can be extended to glial cells as well. In this study, no age-related astrogliosis but decline in microglial cell numbers was found in the motor and sensory cortices. In the same old TNR^{-/-} and TNR^{+/+} mice analysed here, increased numbers of astrocytes and no alterations in microglial cell numbers compared to adult mice have been found in the striatum and cerebellum (Ann-Britt Steen, personal communication). The brain appears to age asynchronously and this has to be considered when designing studies on aging.

5.4 Possible functional significance of the structural aberrations in TNR-deficient mice

Behavioural analyses have revealed that adult TNR-deficient mice have motor deficits and that their neocortex is hyperexcitable. The results of this study show that TNR deficiency leads to aberration in subpopulations of inhibitory neurons in a region- and age-specific fashion. Reduced numbers of calretinin-positive interneurons at adult age might contribute, in an as to yet unknown way, to the dysbalance between excitation and inhibition in the hippocampus and neocortex of TNR deficient mice. The alterations in the size of the parvalbumin- and calretinin-positive interneuron populations in older age might be consequences of functional and structural deficits in these neuronal ensembles already present during adulthood but not detectable with the methods applied here. Future studies combining structural and functional analyses of the same animals may provide valuable new insight into pathophysiological mechanisms underlying brain dysfunctions.

6 SUMMARY

Tenascin-R (TNR) is an extracellular matrix glycoprotein belonging to the tenascin family of proteins. It is expressed by oligodendrocytes, interneurons and motoneurons in the central nervous system. In the adult mouse brain, TNR is found accumulated in perineuronal nets around motoneurons and interneurons and at nodes of Ranvier of myelinated axons. TNR is been implicated in cell adhesion, neurite outgrowth, modulation of ion channels and receptor functions, synaptic plasticity and learning. Constitutive ablation of TNR in mice causes behavioural and physiological abnormalities and impairment of motor coordination. The morphological substrates of the deficits remain largely unknown.

The aim of this study was to analyse quantitatively neuronal and glial cell populations in the motor and sensory cortices of TNR-deficient mice. Densities and numbers per cortical column (cortical tissue under a unit of cortical surface) of immunohistochemically identified major cell types (neurons, neuronal subpopulations, astrocytes, oligodendrocytes and microglia) were stereologically assessed in TNR-deficient mice (TNR^{-/-}) and wild-type (TNR^{+/+}) littermates studied at ages of 5 and 18 months, i.e. adult and old age, respectively.

No differences between TNR^{-/-} and TNR^{+/+} mice at both ages were found for cortical thickness, numbers of all cells and all neurons as well as for oligodendrocytes, astrocytes and microglial cells in both cortical areas. TNR deficiency had an cortical region-specific and age-related impact on the size of subpopulations of interneurons. Calretinin-positive interneurons were already significantly lower in numbers in adult TNR^{-/-} mice compared to wild-type littermates (loss of about -20% in both cortical areas). Calbindin-positive interneuron numbers were normal in adult but reduced in old TNR^{-/-} mice (-23% and -29% compared to TNR^{+/+} mice in the motor and sensory cortex, respectively). Finally, age-related loss of parvalbumin-positive interneurons observed in TNR^{+/+} mice was found to be attenuated in the motor but not the sensory cortex of old TNR^{-/-} animals.

Comparisons of old and adult mice revealed age-related but genotype-independent loss of excitatory neurons, inhibitory parvalbumin-positive interneurons and microglial cells as well as reduction of the total cell numbers and

cortical thickness in the motor area of the neocortex. The magnitude of these age-related changes was between 18% and 44% compared with adult mice. Interestingly, the sensory cortex was less severely affected by aging compared to the motor area in animals of both genotypes: small reduction in the numbers of all neurons (-10% in both genotype groups) and a moderate decrease in the numbers of parvalbumin-positive interneurons (-20% and -31% in TNR^{+/+} and TNR^{-/-} mice, respectively).

The results of this study show that constitutive ablation of TNR does not influence the formation and maintenance throughout life of excitatory neuronal and glial cell populations in the neocortex. Affected by the mutation are subpopulation of interneurons with different functional characteristics and connectivity which may contribute to the previously observed functional deficits in the TNR deficient mouse. Ageing, independent of genotype, appears to influence the motor cortex more than the sensory cortical area. The finding of different degrees of neuronal loss in different neocortical areas is compatible with the differential age-related decline in different cognitive, motor and sensory functions.

7 REFERENCES

- Adams I, Brauer K, Arelin C, Hartig W, Fine A, Mader M, Arendt T, Brückner G (2001) Perineuronal nets in the rhesus monkey and human basal forebrain including basal ganglia. *Neuroscience* 108: 285-298.
- Andersen BB, Gundersen HJ, Pakkenberg B (2003) Aging of the human cerebellum: a stereological study. *J Comp Neurol* 466: 356-365.
- Bartsch U, Pesheva P, Raff M, Schachner M (1993) Expression of janusin (J1-160/180) in the retina and optic nerve of the developing and adult mouse. *Glia* 9:57-69
- Brennecke F, Schachner M, Elger CE, Lie AA (2004) Up-regulation of the extracellular matrix glycoprotein tenascin-R during axonal reorganization and astrogliosis in the adult rat hippocampus. *Epilepsi research* 58(2-3):133-43
- Brennecke F, Bukalo O, Dityatev A, Lie AA (2004) Mice deficient for the extracellular matrix glycoprotein tenascin-R show physiological and structural hallmarks of increased hippocampal excitability, but no increased susceptibility to seizure in the pilocarpine model of epilepsy. *Neurosci* 124(4):841-55
- Brückner G, Grosche J, Hartlage-Rubsamen M, Schmidt S, Schachner M (2003) Region and lamina-specific distribution of extracellular matrix proteoglycans, hyaluronan and tenascin-R in the mouse hippocampal formation. *J Chem Neuroanat* 26: 37-50.
- Brückner G, Grosche J, Schmidt S, Hartig W, Margolis RU, Delpech B, Seidenbecher CI, Czaniera R, Schachner M (2000) Postnatal development of perineuronal nets in wild-type mice and in a mutant deficient in tenascin-R. *J Comp Neurol* 428: 616-629.
- Brückner G, Szeoke S, Pavlica S, Grosche J, Kacza J (2006) Axon initial segment ensheathed by extracellular matrix in perineuronal nets. *Neuroscience* 138: 365-375.
- Carnemolla B, Leprini R, Borsi L, Querze G, Urbini S, Zardi L (1996) Human tenascin-R: complete primary structure, pre-mRNA alternative splicing and gene localization on chromosome 1g23-g24. *J Biol Chem* 271:8157-8160
- Carulli D, Rhodes KE, Brown DJ, Bonnert TP, Pollack SJ, Oliver K, Strata P, Fawcett JW (2006) Composition of perineuronal nets in the adult rat cerebellum and the cellular origin of their components. *J Comp Neurol* 494: 559-577.
- Coggeshall RE, Lekan HA (1996) Methods of Determining Numbers of Cells and Synapses: A Case for More Uniform Standards of Review. *The Journal of Comparative Neurology* 364:6-15
- Dayer AG, Cleaver KM, Abouantoun T, Cameron HA (2005) New GABAergic interneurons in the adult neocortex and striatum are generated from different precursors. *J Cell Biol* 168: 415-427.
- Erickson HP (1993) Tenascin-C, tenascin-R and tenascin-X: a family of talented proteins in search of functions. *Curr Opin Cell Biol* 5:869-876
- Erickson HP (1997) A tenascin knockout with phenotype. *Nature Genet* 17:5-7
- Freitag S, Schachner M, Morelli F (2003) Behavioral alterations in mice deficient for the extracellular matrix glycoprotein tenascin-R. *Behavioural Brain Research* 145:189-207
- Freund TF (2003) Interneuron diversity series: rhythm and mood in perisomatic inhibition. *Trends Neurosci* 26:489-495

- Fukuda T, Kosaka T (2000) The dual network of GABAergic interneurons linked by both chemical and electrical synapses: a possible infrastructure of the cerebral cortex. *Neurosci Res* 38:123-130
- Fuss B, Wintergerst ES, Bartsch U, Schachner M (1993) Molecular characterization and in situ messenger RNA localisation of the neural recognition molecule J1-160/180 – a modular structure similar to tenascin. *J Cell Biol* 120:1237-1249
- Galarreta M, Hestrin S (2002) Electrical and chemical synapses among parvalbumin fast-spiking GABAergic interneurons in adult mouse neocortex. *Proc Natl Acad Sci USA* 99:12438-12443
- Garman RH (1990) Artifacts in routinely immersion fixed nervous tissue. *Toxicol Pathol* 18:149-153
- Gundersen HJ (1986) Stereology of arbitrary particles. A review of unbiased number and size estimators and the presentation of some new ones, in memory of William R. Thompson. *J Microsc* 147 (Pt):3-45
- Gurevicius K, Gureviciene I, Valjakka A, Schachner M, Tanila H (2004) Enhanced cortical and hippocampal neuronal excitability in mice deficient in the extracellular matrix glycoprotein tenascin-R. *Molecular and Cellular Neurosci* 25(3):515-23
- Hof PR, Morrison JH (2004) The aging brain: morphomolecular senescence of cortical circuits. *Trends Neurosci* 27: 607-613.
- Irintchev A, Rosenblatt JD, Cullen MJ, Zweyer M, Wernig A (1998) Ectopic skeletal muscles derived from myoblasts implanted under the skin. *J Cell Sci* 111:3287-3297
- Irintchev A, Salvini TF, Faissner A, Wernig A (1993) Differential expression of tenascin after denervation, damage or paralysis of mouse soleus muscle. *J Neurocytol* 22:955-965
- Irintchev A, Zeschnigk M, Starzinski-Powitz A, Wernig A (1994) Expression pattern of M-cadherin in normal, denervated, and regenerating mouse muscles. *Dev Dyn* 199:326-337
- Jiao Y, Sun Z, Lee T, Fusco FR, Kimble TD, Meade CA, Cuthbertson S, Reiner A (1990) A simple and sensitive antigen retrieval method for free-floating and slide-mounted tissue sections. *J Neurosci* 93:149-162
- Jones FS, Jones PL (1999) The Tenascin Family of ECM Glycoproteins: Structure, Function, and Regulation During Embryonic Development and Tissue Remodeling. *Development Dynamics* 218:235-259
- Lei DL, Long JM, Hengemihle J, O'Neill J, Manaye KF, Ingram DK, Mouton PR (2003) Effects of estrogen and raloxifene on neuroglia number and morphology in the hippocampus of aged female mice. *Neuroscience* 121: 659-666.
- Leprini A, Gherzi R, Siri A, Querze G, Viti F, Zardi L (1996) The human tenascin-R gene. *J Biol Chem* 271:31251-31254
- Lochter A, Schachner M (1993) Tenascin and extracellular matrix glycoproteins: from promotion to polarization of neurite outgrowth in vitro. *J Neurosci* 13:3986-4000
- Long JM, Mouton PR, Jucker M, Ingram DK (1999) What counts in brain aging? Design-based stereological analysis of cell number. *J Gerontol A Biol Sci Med Sci* 54: B407-B417.
- Montag-Sallaz M, Montag D (2003) Severe cognitive and motor coordination deficits in tenascin-R-deficient mice. *Genes, Brain and Behavior* 2(1):20-31
- Morrison JH, Hof PR (1997) Life and death of neurons in the aging brain. *Science* 278: 412-419.

- Mouton PR, Long JM, Lei DL, Howard V, Jucker M, Calhoun ME, Ingram DK (2002) Age and gender effects on microglia and astrocyte numbers in brains of mice. *Brain Res* 956: 30-35.
- Murakami T, Ohtsuka A (2003) Perisynaptic barrier of proteoglycans in the mature brain and spinal cord. *Arch Histol Cytol* 66: 195-207.
- Nikonenko A, Schmidt S, Skibo G, Brückner G, Schachner M (2003) Tenascin-R-deficient mice show structural alterations of symmetric perisomatic synapses in the CA1 region of the hippocampus. *The Journal of Comparative Neurology* 456:338-349
- Packard MG, Knowlton BJ (2002) Learning and memory functions of the Basal Ganglia. *Annu Rev Neurosci* 25:563-93. Epub; 2002 Mar 27.: 563-593.
- Pakkenberg B, Gundersen HJ (1997) Neocortical neuron number in humans: effect of sex and age. *J Comp Neurol* 384: 312-320.
- Pesheva P, Gennarini G, Goriadis C, Schachner M (1993) The F3/F11 cell adhesion molecule mediates the repulsion of neurons by the extracellular matrix glycoprotein J1-160/180. *Neuron* 10:69-82
- Pesheva P, Gloor S, Schachner M, Probstmeier R (1997) Tenascin-R is an intrinsic autocrine factor for oligodendrocyte differentiation and promotes cell adhesion by a sulfatide-mediated mechanism. *J Neurosci* 17:4642-4651
- Saghatelian A, Gorissen S, Albert M, Hertlein B, Schachner M, Dityatev A (2000) The extracellular matrix molecule tenascin-R and its HNK-1 carbohydrate modulate perisomatic inhibition and long-term potentiation in the CA1 region of the hippocampus. *Eur J Neurosci* 12(9):3331-42
- Saghatelian A, de Chevigny A, Schachner M, Lledo PM (2004) Tenascin-R mediates activity-dependent recruitment of neuroblasts in the adult mouse forebrain. *Nature Neurosci*
- Schachner M, Taylor J, Bartsch U, Pesheva P (1994) The perplexing multifunctionality of janusin, a tenascin-related molecule. *Perspect Dev Neurobiol* 2:33-41
- Sofroniew MV, Schrell U (1982) Long-term storage and regular repeated use of diluted antisera in glass staining jars for increased sensitivity, reproducibility, and convenience of single- and two-color light microscopic immunocytochemistry. *J Histochem Cytochem* 30:504-511
- Somogyi P, Klausberger T (2005) Defined types of cortical interneurone structure space and spike timing in the hippocampus. *J Physiol* 562: 91-116.
- Sotelo C (2004) Cellular and genetic regulation of the development of the cerebellar system. *Prog Neurobiol* 72: 295-339.
- Tepper JM, Bolam JP (2004) Functional diversity and specificity of neostriatal interneurons. *Curr Opin Neurobiol* 14: 685-692.
- Teramoto T, Qiu J, Plumier JC, Moskowitz MA (2003) EGF amplifies the replacement of parvalbumin-expressing striatal interneurons after ischemia. *J Clin Invest* 111: 1125-1132.
- Weber P, Bartsch U, Rasband MN, Czaniera R, Lang Y, Bluethmann H, Margolis RU, Levinon SR, Shrager P, Montag D, Schachner M (1999) Mice deficient for tenascin-R display alterations of the extracellular matrix and decreased axonal conduction velocities in the CNS. *J Neurosci* 19(11):4245-4262
- Wegner, F., Hartig, W., Bringmann, A., Grosche, J., Wohlfarth, K., Zuschratter, W. & Brückner, G. (2003) Diffuse perineuronal nets and modified pyramidal cells immunoreactive for glutamate and the GABA(A) receptor alpha1 subunit form a unique entity in rat cerebral cortex. *Exp. Neurol.*, 184, 705-714.

- Wintergerst ES, Fuss B, Bartsch U (1993) Localization of janusin mRNA in the central nervous system of the developing and adult mouse. *Eur J Neurosci* 5: 299-310.
- Xiao ZC, Bartsch U, Margolis RK, Rougon G, Montag D, Schachner M (1997) Isolation of the tenascin-R binding protein from mouse brain membranes. A phosphacan-related chondroitin sulfate proteoglycan. *J Biol Chem* 272(51):32092-101
- Xiao ZC, Revest JM, Laeng P, Rougon G, Schachner M, Montag D (1998) Defasciculation of neurites is mediated by tenascin-R and its neuronal receptor F3/11. *J Neurosci Res* 52(4):390-404
- Yamanaka H, Yanagawa Y, Obata K (2004) Development of stellate and basket cells and their apoptosis in mouse cerebellar cortex. *Neurosci Res* 50: 13-22.
- Zhou FM, Wilson CJ, Dani JA (2002) Cholinergic interneuron characteristics and nicotinic properties in the striatum. *J Neurobiol* 53: 590-605.

8 ABBREVIATIONS

Ab	Antibodies
AEPs	Auditory evoked potentials
CA	Cornu ammon
CaCl ₂	Calcium chloride
CHL1	Close homologue of L1
cm	centimetres
cm ²	Square centrimetres
cm ³	Cubic centrimetres
CNPase	2', 3'-Cyclic Nucleotide 3'-Phosphodiesterase
CNS	Central nervous system
ECM	Extracellular matrix
EEG	Electroenzephalogramm
e.g.	example given
g	gramm
GABA	Gamma amino bytric acid
gt	genotype
Hz	Hertz
i.e.	id est (that is)
Ig	Immunglobulin
kD	kilodalton
KO	Knockout
l	litre
LTP	Long term potentiation
M	Motor cortex
M	molar
m	metre
mm	milimetre (Metre x 10 ⁻³)
ml	millilitre (Litre x 10 ⁻³)
mo	month
ms	milisecond (Second x 10 ⁻³)
NaOH	Sodium hydroxide solution
NaN ₃	Sodium azide
NeuN	Neuron specific nuclear antigen
nm	nanometres
PBS	Phosphate Buffered Saline
pH	p(otential) of H(ydrogen), the logarithm of the reciprocal of hydrogen-ion concentration in gram atoms per litre
PNS	Peripheral nervous system
PPI	Prepulse inhibition
PSA	Poly sialic acid
PV	Parvalbumin
RT	Room temperature
S	Second
S	Sensory Cortex
SD	Standard deviation
v/v	volumne per volumn

WT	wildtype
w/v	weight per volumn
ZMNH	Zentrum für Molekulare Neurobiologie Hamburg
%	Percent
μ	Micro (10^{-6})
μg	Microgramm (gramm x 10^{-6})
μl	Microlitre (Litre x 10^{-6})
°C	Grad Celsius

9 ACKNOWLEDGEMENT/DANKSAGUNG

Die Arbeit wurde am Institut für Biosynthese neuraler Strukturen am Zentrum für molekulare Neurobiologie Hamburg (ZMNH) angefertigt. Bedanken möchte ich mich bei Frau Prof. Dr. Melitta Schachner, die diese Arbeit, als Doktormutter und Direktorin des Institutes, möglich gemacht hat.

Besonders bedanken möchte ich mich bei meinem Betreuer Herrn Dr. Andrey Irintchev, der mir jederzeit für Fragen aller Art zur Verfügung stand und keine Mühe scheute, mir bei dieser Arbeit in jeglicher Hinsicht zu helfen.

Ebenfalls möchte ich mich herzlich bei Frau Emanuela Szpotowicz für das Schneiden und Färben des Mausgewebes bedanken.

Mein besonderer Dank gilt auch Herrn Dr. Gheorghe Tonndorf, der mir helfend zur Seite stand und mich in vielerlei Hinsicht motiviert hat.

Nicht zu vergessen, möchte ich mich bei meinen Eltern Herrn Frank Salis und Frau Anita Salis und bei meiner Schwester Malinde Salis bedanken, die mich über die gesamte Zeit mit Interesse begleitet haben.

10 CURRICULUM VITAE

Personal Data

Family Name	Salis
First Name	Nadine
Date of Birth	09.07.1977
Place of Birth	Hamburg, Germany
Nationality	German
Confession	Protestant

Education

1984-1988	Grundschule Egenbüttel, Rellingen, Germany
1988-1997	Wolfgang-Borchert-Gymnasium, Halstenbek, Germany
1997-2000	Apprenticeship in foreign trade Nordmann, Rassmann GmbH & Co., Hamburg, Germany
2000-2006	Regular student of medicine Universität Hamburg, Germany

11 EIDESSTATTLICHE VERSICHERUNG

Ich versichere ausdrücklich, dass ich die Arbeit selbständig und ohne fremde Hilfe verfasst, andere als die von mir angegebenen Quellen und Hilfsmittel nicht benutzt und die aus den benutzten Werken wörtlich oder inhaltlich entnommenen Stellen einzeln nach Ausgabe (Auflage und Jahr des Erscheinens), Band und Seite des benutzten Werkes kenntlich gemacht habe.

Ferner versichere ich, dass ich die Dissertation bisher nicht einem anderem Fachvertreter an einer anderen Hochschule zur Überprüfung vorgelegt oder mich anderweitig um Zulassung zur Promotion beworben habe.

Nadine Salis